DMD Fast Forward. Published on January 17, 2014 as doi:10.1124/dmd.113.054767
This article has not been copyedited and formatted. The final version may differ from this version.

DMD #54767

Interaction of novel platelet-increasing agent eltrombopag with rosuvastatin via breast cancer resistance protein in human

Kazuya Takeuchi, Tomoko Sugiura, Kazuki Matsubara, Ren Sato, Takuya Shimizu, Yusuke Masuo, Masato Horikawa, Noritaka Nakamichi, Norihisa Ishiwata and Yukio Kato

Faculty of Pharmacy, Institute of Medical, Pharmaceutical and Health Sciences, Kanazawa University, Kanazawa 920-1192, Japan (K.T., T.S., K.M., R.S., T.S., Y.M., N.N., Y.K.) and Pharmaceutical Research Department, Biological Research Laboratories, Nissan Chemical Industries, Ltd., Saitama 349-0294, Japan (K.T., M.H., N.I.)

Running title:

Interaction of eltrombopag with rosuvastatin via BCRP

Corresponding author:

Prof. Yukio Kato, Ph.D

Faculty of Pharmacy, Institute of Medical, Pharmaceutical and Health Sciences,

Kanazawa University

Kakuma-machi, Kanazawa 920-1192, Japan

Tel/Fax:(81)-76-234-4465 / Email: ykato@p.kanazawa-u.ac.jp

Document statistics:

number of text pages: 40

number of tables: 2

number of figures: 7

number of references: 33

number of words:

Abstract: 247

Introduction: 739

Discussion: 1498

Abbreviations:

ABC, ATP binding cassette; BCRP, breast cancer resistance protein; ELT, eltrombopag; HEK, human embryonic kidney; ITP, idiopathic thrombocytopenic purpura; OATP, organic anion-transporting polypeptide; OCT, organic cation transporter; PBPK, physiologically based pharmacokinetic;

ABSTRACT

Eltrombopag (ELT), an orally available thrombopoietin receptor agonist, is a substrate of organic anion transporting polypeptide (OATP) 1B1, and coadministration of ELT increases the plasma concentration of rosuvastatin in humans. Since the pharmacokinetic mechanism(s) of the interaction is unknown, the present study aimed to clarify the drug interaction potential of ELT at transporters. The OATP1B1-mediated uptake of ELT was inhibited by several therapeutic agents used to treat lifestyle diseases. Among them, rosuvastatin was a potent inhibitor with the concentration for half-maximal inhibition (IC_{50}) of 0.05 μM, which corresponds to 1/7th of the calculated maximum unbound rosuvastatin concentration at the inlet to the liver. Nevertheless, a simulation study using a physiologically based pharmacokinetic (PBPK) model predicted that the effect of rosuvastatin on the pharmacokinetic profile of ELT *in vivo* would be minimal. On the other hand, ELT potently inhibited uptake of rosuvastatin by OATP1B1 and human hepatocytes with an IC_{50} of 0.1 μM. However, the results of simulation study indicated that inhibition of OATP1B1 by ELT can only partially explain the clinically observed interaction with rosuvastatin. ELT also inhibited transcellular transport of rosuvastatin in MDCKII cells stably expressing breast cancer resistance protein (BCRP), and was found to be a substrate of BCRP. The interaction of ELT with rosuvastatin can be almost quantitatively explained on the assumption that intestinal secretion of rosuvastatin is essentially completely inhibited by ELT. These results suggest that BCRP in small intestine may be the major target for interaction between ELT and rosuvastatin in humans.

DMD Fast Forward. Published on January 17, 2014 as DOI: 10.1124/dmd.113.054767
This article has not been copyedited and formatted. The final version may differ from this version.

INTRODUCTION

Eltrombopag (ELT) is an orally available, small-molecular, non-peptide thrombopoietin receptor agonist (Erickson-Miller *et al.*, 2004; Sellers *et al.*, 2004; Jenkins *et al.*, 2007; Bussel *et al.*, 2007) that has been approved worldwide (Promacta® / Revolade®) for the treatment of idiopathic thrombocytopenic purpura (ITP). ELT interacts with the transmembrane domain of the thrombopoietin receptor (Erickson-Miller *et al.*, 2008) and activates intracellular signal transduction pathways, leading to stimulation of the proliferation and differentiation of megakaryocytes and progenitor cells in bone marrow, thereby resulting in an increase of platelets in the circulating blood. Further clinical trials of ELT are ongoing for treatment of cancer chemotherapy-induced thrombocytopaenia and hepatitis C-induced thrombocytopaenia. Thus, the potential clinical importance of ELT is substantial.

Due to the decrease in platelets, ITP induces severe symptoms, including intracerebral bleeding. ELT is expected to prevent such bleeding symptoms by inducing a recovery of platelet numbers. On the other hand, overdose of ELT may lead to activation of the blood coagulation system, which in turn may promote thromboembolism （Cheng *et al.*, 2011）. Therefore, it is important to maintain systemic plasma concentration of ELT at the optimum level. In addition, pharmacotherapy with ITP requires long-term treatment （Stasi *et al.*, 2004）. This may increase the likelihood that ELT will be coadministered with other therapeutic agents. Thus, it is very important to consider potential drug interactions that might unexpectedly increase or decrease the systemic concentration of ELT. Nevertheless, only limited information is available on pharmacokinetic mechanism(s) of ELT and the potential for interaction with other drugs.

ELT is minimally excreted into urine after oral administration in humans, suggesting that the major clearance organ is the liver (Bauman *et al*., 2011). According to our previous study, hepatic uptake could be the rate-limiting process in the overall elimination of

ELT (Takeuchi *et al.*, 2011). Hepatic uptake of ELT is mediated at least in part by organic anion transporting peptide (OATP) 1B1 (Takeuchi *et al.*, 2011) although the contribution of this transporter to hepatic ELT uptake remains to be precisely clarified. Nevertheless, certain drugs such as gemfibrozil, rifampicin and cyclosporin A are known to interact in a clinically significant way with OATP1B1-mediated hepatic uptake of therapeutic agents in humans (Kalliokoski *et al.*, 2010). OATP1B1 recognizes a wide range of substrate drugs, including anti-hyperlipidemic agents such as HGM-CoA reductase inhibitors and anti-diabetic agents such as repaglinide and nateglinide (Kitamura *et al*., 2008, Kalliokoski *et al*., 2008). Therefore, these drugs may also inhibit OATP1B1-mediated hepatic uptake of other substrate drugs, including ELT. It should be noted that these drugs are commonly used for the treatment of lifestyle diseases and, therefore, are quite likely to be coadministered with ELT in the clinical situation. Thus, it is important to quantitatively assess the interaction potential of these drugs with hepatic uptake of ELT via transporters.

Interaction potential of ELT as a perpetrator drug with other therapeutic agents has already been clinically reported. Allred *et al.* (2011) reported that the plasma concentration of rosuvastatin was increased by concomitant administration of ELT, whereas rosuvastatin did not affect the plasma concentration of ELT. ELT can act as an inhibitor of OATP1B1, at least in gene-transfected cell lines *in vitro* (Takeuchi *et al.*, 2011). Because rosuvastatin is mainly eliminated from the liver (Martin *et al.*, 2003), and its hepatic uptake process is primarily mediated by OATP1B1 (Kitamura *et al*., 2008), the interaction by ELT is considered to involve the OATP1B1-mediated hepatic uptake process, though the details remain unclear.

Drug interactions could thus be a critical issue in clinical use of ELT. Quantitative assessment of possible interactions between ELT and concomitantly administered drugs is urgently required to ensure safe administration of ELT to patients. In the present study, we first investigated the inhibitory effect of various therapeutic agents, including statins, on

OATP1B1-mediated uptake of ELT. Physiologically based pharmacokinetic (PBPK) analysis was performed to quantitatively assess the interaction via OATP1B1 in humans. We focused particularly on the clinically reported interaction of ELT with rosuvastatin (Allred *et al.*, 2011). However, although ELT potently inhibits OATP1B1-mediated uptake of rosuvastatin in human hepatocytes *in vitro,* PBPK analysis indicated that such an interaction is unlikely to be significant *in vivo*. Instead, ELT was found to be a potent inhibitor of breast cancer resistance protein (BCRP), an ATP binding cassette (ABC) efflux transporter. Our results indicate that BCRP in the small intestine could be the major site of interaction between ELT and rosuvastatin in humans *in vivo*.

MATERIALS AND METHODS

Materials

ELT was synthesized by Nissan Chemical Industries, Ltd. (Tokyo, Japan). Rosuvastatin was purchased from Toronto Research Chemicals Inc. (Ontario, Canada). Rhodamine 123 was purchased from Tokyo Chemical Industry Co., Ltd. (Tokyo, Japan). Cryopreserved human hepatocytes (H1000.H15T, #694, from a 29-year-old male Causasian; [XenoTech, Lenexa, KS]) were obtained from Sekisui Medical (Tokyo, Japan). Cryopreserved hepatocyte purification kit (454500) was purchased from Becton, Dickinson (Franklin Lakes, NJ). All other chemicals and reagents were of analytical grade and were obtained from commercial sources.

Animals

Six- to 9-week-old male *mdr1a/1b/bcrp*$^{-/-}$ and FVB mice were purchased from Taconic (Germantown, NY, USA) and CLEA Japan Inc. (Tokyo, Japan), respectively. The mice were kept in a temperature- and light-controlled environment with standard food and tap water provided ad libitum. Animal experiments were carried out in accordance with the Guide for the Care and Use of Laboratory Animals at the Takara-machi Campus of Kanazawa University.

Pharmacokinetic Studies in Mice

Mice were fasted overnight with free access to water and anesthetized with diethylether during drug administration and blood sampling. ELT was dissolved in saline containing 5 μM human serum albumin (HSA) to obtain a final concentration of 0.4 mg/mL and orally administered by gavage (2 mg/kg body weight). This concentration of albumin fully suppresses non-specific adsorption of ELT on the experimental apparatus (Takeuchi et

al., 2011). Rosuvastatin was prepared in 0.5% hydroxypropyl methylcellulose for oral administration by gavage (10 mg/5 mL/kg body weight) and in saline containing 5 μM HSA for intravenous administration via the tail vein (4 mg/2 mL/kg body weight). At various intervals after administration, blood samples were collected through the caudal vein. All blood samples were immediately centrifuged to obtain plasma, which was used for quantitation.

In the closed loop study, mice were fasted for about 6 hours with free access to water and anesthetized with intraperitoneal injection of pentobarbital. The abdomen was opened, and a 10-cm closed loop from just below the duodenal papilla was prepared by ligating both ends of the gut. ELT (2 mg/1 mL/kg body weight) or water (1 mL/kg body weight) was injected into the intestinal loop. At 1 min after the administration, rosuvastatin (10 mg/5 mL/kg body weight) was also injected into the intestinal loop. The intestinal loop was returned to the abdominal cavity, and the abdomen was closed with sutures. At various intervals after rosuvastatin administration, blood samples were collected through the jugular vein, followed by immediate centrifugation to obtain plasma. The body temperature was maintained by placing the animals on a thermostated heating pad.

Cell Culture and Transport Studies in HEK293 Cells expressing OATP1B1 and organic cation transporter (OCT) 1

HEK293 cells stably expressing full-length OATP1B1 (HEK293/OATP1B1 cells) were previously constructed (Fujita *et al*., 2014) and HEK293/OCT1 cells were constructed in the present study by transfecting HEK293 cells with pcDNA3 vector (Invitrogen, Carlsbad, CA) into which full-length human OCT1 gene had been subcloned, using the calcium phosphate precipitation method. HEK293/OCT1 cells were then selected by adding G418 (1 mg/mL, Wako Pure Chemical) to the medium and grown in D-MEM without L-glutamine or

phenol red (Wako Pure Chemical) containing 10% fetal bovine serum, penicillin, streptomycin and G418 in a humidified incubator at 37°C under an atmosphere of 5% CO_2 in air. For HEK293/OATP1B1 cells, after the cells had reached confluence, they were harvested and suspended in ice-cold transport buffer (pH 7.4; Sugiura *et al*., 2010). The uptake experiment for ELT in HEK293/OATP1B1 was performed in the presence of 5 μM HSA, and the ELT uptake was measured according to the silicone oil layer method (Sugiura *et al*., 2010). Free fractions of ELT, rosuvastatin, and atorvastatin in the transport buffer containing 5 μM HSA were determined by equilibrium dialysis method using the BD Gentest™ Serum Binding System (Becton, Dickinson and Company, Franklin Lakes, NJ). The uptake experiment for rosuvastatin was performed in the absence of HSA, and ELT concentration in the medium was directly measured by LC/MS/MS. In the inhibition study, the inhibitor was added to cell suspension simultaneously with the substrate. In the case of HEK293/OCT1 cells, they were cultured in poly-L-lysine-coated 12-well plates and directly used for uptake study (Takeuchi *et al*., 2011). The cellular protein content was determined according to the Bradford method using a protein assay kit (Bio-Rad Laboratories, Hercules, CA) with bovine serum albumin as the standard.

Transport Studies in Human Cryopreserved Hepatocytes

Cryopreserved human hepatocytes were prepared using a cryopreserved hepatocyte purification kit. The hepatocytes were resuspended in the transport buffer to give a cell density of 1.0 x 10^6 cells/mL. We checked cell viability by means of a trypan blue exclusion test and used hepatocytes showing more than 90% viability. The uptake experiment was then performed according to the silicone oil layer method (Takeuchi *et al*., 2011) with some modifications. In brief, 350 μL of the cell suspension was preincubated for 5 min at 37˚C, then the reaction was started by mixing the suspension with an equal volume of prewarmed

transport buffer containing rosuvastatin with or without ELT. At appropriate times, 200 µL aliquots of the mixture were withdrawn and quickly centrifuged through a silicone oil layer (density, 1.015) to separate the cells from the transport buffer. Then, 50 µl aliquots of the supernatant (upper layer) were immediately removed and mixed with an equal volume of the transport buffer containing 0.5 v/v% Tween 80 to avoid non-specific adsorption of ELT. The hepatocytes (lower layer) were incubated overnight in alkali (0.75 N KOH) to dissolve the hepatocytes. Both the upper and lower layers were stored at -30˚C until LC/MS/MS analysis for determination of rosuvastatin uptake and medium concentration of ELT.

Transport Studies with MDCKII/BCRP/PDZK1 Cells

MDCKII cells stably expressing both BCRP and PDZK1 (MDCKII/BCRP/PDZK1 cells) and those stably expressing PDZK1 alone (MDCKII/Mock/PDZK1) were previously obtained (Shimizu et al., 2011), and were grown in Dulbecco's modified Eagle's medium containing 10% fetal calf serum, penicillin, streptomycin, 1 mg/mL G418 and 0.2 mg/mL zeocin in a humidified incubator at 37˚C under an atmosphere of 5% CO_2 in air. MDCKII/BCRP/PDZK1 and MDCKII/Mock/PDZK1 cells were seeded in Transwell polycarbonate inserts (3 µm pore size, 12 mm diameter; Corning Life Science, Edison, NJ) at a density of 3 x 10^5 cells/well. After 3 days of culture, the cell monolayers were washed twice with the transport buffer including 5 µM HSA. The same buffer also containing ELT or rosuvastatin with or without inhibitors was added to the basal (BL) or apical (AP) chamber. At the designated times, a 100-µL aliquot was sampled from the opposite side and replaced with an equal volume of prewarmed fresh buffer.

The efflux ratio (ER) was calculated as the ratio of the apparent permeability coefficient (P_{app}) in the BL-to-AP direction to that in the AP-to-BL direction, where P_{app} was calculated as the slope of the regression line in the transport-time profile of the drug divided

DMD Fast Forward. Published on January 17, 2014 as DOI: 10.1124/dmd.113.054767
This article has not been copyedited and formatted. The final version may differ from this version.

by the initial drug concentration in the donor chamber and the cell monolayer surface area (1.1 cm^2). The net flux ratio was calculated as follows:

$$Net\ flux\ ratio = \frac{ER_{BCRP}}{ER_{Mock}} \quad (1)$$

Uptake Studies with LLC-PK1 and LLC-GA5-COL150 cells

LLC-PK1 cells and LLC-GA5-COL150 cells stably expressing P-glycoprotein (Tanigawara *et al*., 1992; Ueda *et al*., 1992) were obtained from Riken Cell Bank (Tsukuba, Japan), and were cultured and grown in medium 199 containing 10% fetal calf serum, penicillin and streptomycin in a humidified incubator at 37˚C under an atmosphere of 5% CO_2 in air. For LLC-GA5-COL150 cells, 150 ng/mL colchicine was added to ensure stable expression of P-glycoprotein. LLC-PK1 cells and LLC-GA5-COL150 cells were seeded on 24-well plates at densities of 0.5 x 10^5 cells/well and 5.7 x 10^5 cells/well, respectively. After 3 days of culture, LLC-GA5-COL150 cells were cultured without colchicine for 6 hours. Then LLC-PK1 cells and LLC-GA5-COL150 cells were washed twice with the transport buffer and pre-incubated with the same buffer for 30 minutes. After the pre-incubation, the transport buffer containing substrate and inhibitor with 5 μM HSA was added and incubation was continued for 90 minutes. Cells were then washed twice with ice-cold buffer. To determine uptake of rhodamine 123, cells were lysed with 10 mM KH_2PO_4 buffer (pH 7.4) containing 0.1% Triton X-100, and the cellular protein content was determined by using a BCA protein assay kit (Thermo Scientific, Rockford, IL), which was chosen in order to avoid interference from the absorbance spectrum of Triton X-100. Rhodamine 123 in the cell lysate and medium was quantified with a microplate fluorometer (MTP-880Lab, Hitachi High-Tech, Tokyo, Japan) with excitation and emission of 490 and 530 nm, respectively. To determine uptake of rosuvastatin, cells were lysed with 0.2 N NaOH, and rosuvastatin in the cell lysate and medium was quantified by LC/MS/MS. Uptakes of rhodamine 123 and rosuvastatin were

DMD Fast Forward. Published on January 17, 2014 as DOI: 10.1124/dmd.113.054767
This article has not been copyedited and formatted. The final version may differ from this version.

normalized by both cellular protein amount and substrate concentration in the medium.

Liquid Chromatography

Quantification of ELT and rosuvastatin was performed using a triple quadrupole mass spectrometer with electrospray ionization (ESI) (Quattro Premier XE, Waters Corporation, Milford, MA) coupled to a liquid chromatography system (ACQUITY UPLC, Waters Corporation). Chromatography was performed by means of step-gradient elution (flow rate, 0.5 mL/min) as follows: 0 to 0.4 min, 65% A/ 35% B; 0.4 to 3.6 min, 65% A/ 35% B to 5% A/95% B; 3.6 to 4.6 min, 5% A/ 95% B; 4.6 to 5.5 min, 65% A/ 35% B (A, 0.1% formic acid; B, acetonitrile/methanol (3:2) containing 0.1% formic acid) using an ACQUITY UPLC BEH Shield RP_{18} (1.7 μm particle size, 2.1 mm I.D.×50 mm; Waters Corporation) at 45°C for ELT, and 0 to 2.0 min, 95% A/ 5% B to 5% A/95% B; 2.0 to 3.0 min, 5% A/ 95% B; 3.0 to 3.5 min, 95% A/ 5% B (A, 0.1% formic acid; B, acetonitrile containing 0.1% formic acid) using an ACQUITY UPLC BEH C_{18} (1.7 μm particle size, 2.1 mm I.D.×50 mm; Waters Corporation) at 45°C for rosuvastatin. The multiple reaction monitor was set at 443.2 to 228.6 m/z for ELT, 482.1 to 258.1 m/z for rosuvastatin, and 295.9 to 214.7 m/z for I.S. (diclofenac). The quantitation limit was 10 ng/mL (20 nM) for ELT and 5 ng/mL (10 nM) for rosuvastatin. Determination of metformin, cimetidine and ranitidine was performed using an HPLC system consisting of a model LC-10AD VP pump and a model SPD-10A VP UV monitor (Shimadzu, Tokyo, Japan) with a COSMOSIL $5C_{18}$-AR-II column (4.6 mm I.D.×150 mm; Nacalai Tesque, Kyoto, Japan) for metformin or $5C_{18}$-MS-II column (4.6 mm I.D.×150 mm; Nacalai Tesque) for cimetidine and ranitidine. For metformin, the mobile phase consisted of 20 mM ammonium acetate containing 2.5 mM 1-octanesulfonic acid sodium salt/methanol (85:15) at the flow rate of 1 mL/min. The wavelength of UV detection was at 236 nm. For cimetidine and ranitidine, the mobile phase consisted of 10 mM potassium phosphate (pH

8.0)/acetonitrile (90:10 for cimetidine, 88:12 for ranitidine) at the flow rate of 1 mL/min. The wavelength of UV detection was set at 228 nm.

Data Analysis

Concentration-dependent inhibition of the uptake by an inhibitor was fitted to the following equation to estimate the concentration for half-maximal inhibition (IC_{50}):

$$R = IC_{50}^{n}/(IC_{50}^{n} + I^{n}) \quad (2)$$

where R, I and n are the uptake normalized by the control (without inhibitor) value, the inhibitor concentration and Hill's coefficient, respectively. Statistical analysis was performed by using Student's *t* test. A difference between means was considered to be significant when $p < 0.05$.

Assessment of Drug Interaction Potential Based on Static Model

The IC_{50} of therapeutic agents for OATP1B1-mediated uptake of ELT or rosuvastatin was compared with their maximum plasma concentration ($C_{max,sys}$) or maximum concentration at the inlet to the liver ($C_{max,pv}$) in humans. The $C_{max,sys}$ values were taken from the interview forms of the therapeutic agents (CRESTOR®, Lipitor®, MEVALOTIN®, SUREPOST®, Starsis®, EUGLUCON®, Predomine®, Clarith®, Sawacillin®, Omepral®, Pariet®, Takepron®, AZANIN®, Endoxan® and Revolade®) and $C_{max,pv}$ was calculated according to the following equation (Ito *et al.*, 1998):

$$C_{\max,\,pv} = C_{\max,\,sys} + \frac{F_a \bullet k_a \bullet Dose}{Q_h} \quad (3)$$

where F_a, k_a and Q_h represent fraction absorbed, first-order absorption rate and hepatic blood flow, respectively. The values of F_a and k_a were assumed to be 1 and 0.1, respectively (Ito *et al.*, 1998), whereas Q_h was fixed to be 1450 mL/min (Davies et al., 1993, Table 1).

DMD Fast Forward. Published on January 17, 2014 as DOI: 10.1124/dmd.113.054767
This article has not been copyedited and formatted. The final version may differ from this version.

Fitting and Simulation based on PBPK Model

To understand the clinically observed drug interaction between rosuvastatin and ELT (Allred *et al.*, 2011), the PBPK model shown in supplementary Figure S1 was constructed. The mass-balance equations deduced from the model are also shown in Figure S1, where X_g, $C_{ext,B}$, C_B and C_{liver} are the amount of drug in the GI tract, blood concentration in hepatic extracellular space, systemic blood concentration and hepatic concentration, respectively. It was assumed that (i) only the systemic blood and liver need to be considered as distribution organs, since both compounds are primarily distributed to the liver (Martin *et al.*, 2003; Bauman *et al.*, 2011); (ii) hepatic elimination is primarily mediated by the influx process without back flux from the liver to extracellular space, since hepatic uptake is rate-limiting for both compounds （Jones *et al.*, 2012; Takeuchi *et al*, 2011）; (iii) the plasma concentration profile is evaluated over a sufficiently short time period that enterohepatic circulation can be neglected. Fraction orally absorbed ($F_a \cdot F_g$), blood-to-plasma partition coefficient (R_b), plasma unbound fraction (f_p) and non-hepatic clearance (CL_{NH}) of rosuvastatin and ELT were obtained from the literature (FDA Pharmacology Review of Promacta; Martin *et al.*, 2003, Table 1). The volume of extracellular space in liver (V_{extra}) and volume of liver (V_{liver}) were also taken from the literature (Table 1, Davies *et al.*, 1993; Watanabe *et al.*, 2009). The k_a, distribution volume (V_d) and intrinsic clearance for hepatic uptake (PS_{inf}) were estimated in the present study by simultaneous nonlinear least-squares fitting of the model to the blood concentration profiles of each compound (without coadministered drugs) reported previously (Deng *et al.*, 2011; Allred *et al.*, 2011) using the nonlinear regression analysis program Napp (Ver 2.3.1 for Macintosh OS-X, The University of Tokyo Hospital), where the blood concentration was obtained as the product of plasma concentration and R_b.

To simulate plasma concentration profile in the presence of coadministered drug,

DMD Fast Forward. Published on January 17, 2014 as DOI: 10.1124/dmd.113.054767
This article has not been copyedited and formatted. The final version may differ from this version.

the apparent intrinsic clearance for hepatic uptake ($PS_{inf,app}$) was defined according to the following equation:

$$PS_{inf,app} = \frac{PS_{inf}}{(1 + \frac{f_p \bullet C_{ext,B} / R_B}{K_i})} \quad (4)$$

where K_i represents the inhibition constant. In deriving Eq. (4), we assumed that hepatic uptake is primarily mediated by OATP1B1, which is inhibited by the coadministered drug. Therefore, K_i was set to be the IC_{50} obtained from the uptake study in HEK293/OATP1B1 cells. When we simulated the inhibition of intestinal secretion by coadministered drug, $F_a \cdot F_g$ was assumed to be close to unity. The simulation was performed using the Napp program.

DMD Fast Forward. Published on January 17, 2014 as DOI: 10.1124/dmd.113.054767
This article has not been copyedited and formatted. The final version may differ from this version.

RESULTS

Effects of Therapeutic Agents on OATP1B1-mediated ELT Uptake

The inhibitory effects of various types of drugs, including those for ITP and lifestyle diseases, on ELT uptake by OATP1B1 were examined in HEK293/OATP1B1 cells. OATP1B1-mediated uptake of ELT was decreased in the presence of rosuvastatin, atorvastatin, repaglinide, nateglinide, glibenclamide and clarithromycin (Figure 1A and 1B). Inhibition by rosuvastatin and atorvastatin was particularly potent, and they had the lowest IC_{50} values (Table 2). Inhibitory effects of repaglinide, nateglinide, glibenclamide and clarithromycin were less potent, but appeared to be concentration-dependent (Figure 1A and 1B). Note that the IC_{50} values could be apparent values since the inhibition study was performed in the presence of 5 μM HSA (see Methods), which is essential to assess OATP1B1-mediated uptake of ELT in order to minimize nonspecific adsorption (Takeuchi *et al.* 2011). Therefore, unbound fraction of rosuvastatin and atorvastatin in the transport buffer containing HSA was measured by equilibrium dialysis, and the IC_{50} in terms of the unbound concentration was also determined. The obtained IC_{50} values for rosuvastatin and atorvastatin were 47 and 28 nM, respectively (Table 2).

Assessment of Drug Interaction Potential by Therapeutic Agents

We next attempted to assess possible inhibition of OATP1B1-mediated ELT uptake by these therapeutic agents *in vivo*, using both static and dynamic (PBPK) models. In the static model, the IC_{50} obtained in the present study was compared with $C_{max,sys}$ and $C_{max,pv}$ (Table 2). For all drugs except rosuvastatin and atorvastatin, both $C_{max,sys}$ and $C_{max,pv}$ were much lower than the IC_{50} value (Table 2). On the other hand, unbound $C_{max,pv}$ of rosuvastatin and atorvastatin was higher than the IC_{50} value defined in terms of the unbound concentration (Table 2), indicating possible inhibition of OATP1B1-mediated hepatic uptake of ELT *in vivo*.

DMD Fast Forward. Published on January 17, 2014 as DOI: 10.1124/dmd.113.054767
This article has not been copyedited and formatted. The final version may differ from this version.

However, this was in conflict with the clinical finding that the plasma concentration of ELT was not affected by rosuvastatin (Allred *et al*. 2011). Therefore, to estimate drug interaction potential more quantitatively, we simulated plasma concentration-time profiles based on the PBPK model (Figure S1). First, the PBPK model was fitted to plasma concentrations after oral administration of ELT alone (75 mg, Deng *et al.*, 2011) to estimate k_a, V_d and PS_{inf} of ELT (shown in Table 1). The fitted line was almost superimposed on the observed data (Figure 2A, solid line). Similarly, the PBPK model was fitted to the plasma concentration profile after oral administration of rosuvastatin alone (10 mg, Allred *et al.*, 2011) to estimate k_a, V_d and PS_{inf} of rosuvastatin (Table 1). The fitted line thus obtained was in good agreement with the observed data (Figure 2B, solid line). Next, using $PS_{inf,app}$ calculated according to Eq. 4, we simulated the plasma concentration of ELT when rosuvastatin was simultaneously administered. The simulated plasma concentration-time profile of ELT was not greatly changed from the control (ELT alone, Figure 2A). Thus, the present simulation was in agreement with the clinical findings (Allred *et al.*, 2011). We also performed sensitivity analysis, simulating the plasma ELT profile for the case that IC_{50} *in vivo* was 1/3rd or 1/10th of that obtained *in vitro*, but again, the simulated plasma concentration was not remarkably different from the control (Figure 2A).

Effect of ELT on Hepatic Uptake of Therapeutic Agents

We next focused on the clinically observed interaction of ELT with rosuvastatin (Allred *et al.*, 2011). Since rosuvastatin is excreted mainly from the liver (Martin et al., 2003), the effect of ELT on hepatic uptake of rosuvastatin was first examined using cryopreserved human hepatocytes. Rosuvastatin uptake by human hepatocytes was inhibited by ELT in a concentration-dependent manner (Figure 3A, IC_{50} ~ 0.11 μM). Since rosuvastatin and ELT are OATP1B1 substrates, we also investigated the effect of ELT on uptake of rosuvastatin in

HEK293/OATP1B1 cells. OATP1B1-mediated uptake of rosuvastatin was also inhibited by ELT in a concentration-dependent manner (Figure 3B), the obtained IC_{50} being close to that obtained in human hepatocytes (Table 2). These experiments were performed in the absence of HSA. Therefore, to eliminate the influence of nonspecific adsorption of ELT on the experimental apparatus, we directly measured the medium concentration of ELT in both human hepatocytes and HEK293/OATP1B1 cells; the IC_{50} values for ELT shown in Table 2 were defined in terms of observed ELT concentration in the medium. Alternatively, if we use ELT concentration added to the medium, the calculated IC_{50} was 2.0 μM which leads to approximately 20-fold underestimation of its inhibitory potency. Thus, care is needed in assessing potential inhibition by highly adsorbed compounds such as ELT.

ELT is also a substrate and inhibitor of OCT1, so the inhibitory effect of ELT on uptake of OCT1 substrate drugs, metformin, ranitidine and cimetidine (Bourdet *et al.*, 2005, Kimura *et al.*, 2005), was examined in HEK293/OCT1 cells. OCT1-mediated uptake of cimetidine was minimally inhibited by ELT, whereas that of metformin was inhibited in a concentration-dependent manner with an IC_{50} value of 39 μM (Figure 3C). Unbound fraction of ELT in the transport buffer containing HSA was measured, and the IC_{50} defined in terms of the unbound ELT concentration was found to be 0.28 μM. This IC_{50} is higher than unbound $C_{max,sys}$ and $C_{max,pv}$ of ELT (Table 2).

Next, to quantitatively explain the drug interaction between ELT and rosuvastatin *in vivo* in humans, the plasma concentration of rosuvastatin coadministered with ELT was simulated based on the PBPK model using $PS_{inf,app}$ estimated according to Eq. 4. The simulated plasma concentration profile of rosuvastatin was not much different from that after oral administration of rosuvastatin alone (Figure 2B). According to this simulation, the increase of AUC and C_{max} for rosuvastatin caused by coadministration of ELT amounted to just 24% and 21%, respectively, compared with those after administration of rosuvastatin

alone (Figure 2B). This explains only a part of the clinically reported interaction (the increase amounted to 55% and 103% for AUC and C_{max}, respectively; Allred et al., 2011). The simulated plasma concentration became more consistent with the clinical data only if we assumed that IC_{50} *in vivo* was 1/3rd or 1/10th of that obtained *in vitro* (Figure 2B).

Interaction of ELT with ABC transporters in small intestine

We next focused on the secretion process of rosuvastatin as a possible target for the clinically observed interaction with ELT. In the liver, rosuvastatin is secreted into the bile via multiple ABC transporters (Kitamura *et al.*, 2008). Intestinal secretion of rosuvastatin may also be governed by ABC transporters (Keskitalo *et al.*, 2009). Therefore, as the first step to study possible involvement of ABC transporters in the interaction between ELT and rosuvastatin, the pharmacokinetic studies using *mdr1a/1b/bcrp*$^{-/-}$ mice were conducted to simultaneously evaluate the effect of ELT on the two ABC transporters, BCRP and P-glycoprotein. Involvement of BCRP and/or P-glycoprotein in intestinal secretion of rosuvastatin was supported by the present finding that the plasma concentration profile of rosuvastatin after oral administration in *mdr1a/1b/bcrp*$^{-/-}$ mice was much higher than that in wild-type mice (Figure 4A), whereas the difference in plasma concentration profile between the two strains was not so marked after intravenous administration of rosuvastatin (Figure 4B). Plasma concentration of ELT after oral administration in *mdr1a/1b/bcrp*$^{-/-}$ was also much higher than that in wild-type mice (Figure 4C), suggesting that ELT also interacts with these ABC transporters.

To examine possible interaction of ELT with intestinal absorption of rosuvastatin, the plasma concentration-time profile of rosuvastatin was examined after injection of rosuvastatin into an intestinal loop with or without ELT. The plasma concentration of rosuvastatin after coadministration with ELT was higher than that after injection of

rosuvastatin alone (Figure 5). The present study was limited to pharmacokinetic interaction, but the interaction in terms of clinical endpoints was not analyzed because ELT is able to increase the platelet count only in human and chimpanzee (Erickson-Miller *et al.*, 2008) whereas HMG-CoA reductase inhibitors do not show the LDL lowering effect in rodents (Fujioka *et al.*, 1995).

Interaction of ELT with BCRP, but not P-glycoprotein

Since the interaction of ELT with rosuvastatin cannot be fully explained by the interaction at the hepatic uptake process (Figure 2B), we speculated that interaction might also occur at BCRP or P-glycoprotein. To clarify the inhibitory effect of ELT on BCRP-mediated transport of rosuvastatin, we examined transcellular transport of rosuvastatin across MDCKII/BCRP/PDZK1 cells. Transport of rosuvastatin in the AP-to-BL direction across MDCKII/BCRP/PDZK1 cells was lower than that across MDCKII/mock/PDZK1 cells (Figure 6A). In the presence of 10 μM ELT, transport of rosuvastatin in the AP-to-BL direction across MDCKII/BCRP/PDZK1 cells was elevated and became similar to that across MDCKII/mock/PDZK1 cells (Figure 6A). Next, bidirectional transport of rosuvastatin was measured in the presence of various concentrations of ELT in both cells to determine the net flux ratio of rosuvastatin. We found that the net flux ratio was decreased by ELT in a concentration-dependent manner (Figure 6B).

To further support the interaction of ELT with BCRP, transcellular transport of ELT by BCRP was also examined. Transport of ELT in the AP-to-BL direction across MDCKII/BCRP/PDZK1 cells was lower than that across MDCKII/mock/PDZK1 cells (Figure 7A). In the presence of 1 μM Ko143, an inhibitor of BCRP, transport of ELT in the AP-to-BL direction across MDCKII/BCRP/PDZK1 cells was elevated and became similar to that across MDCKII/mock/PDZK1 cells (Figure 7A). Bidirectional transport of ELT was then

measured at various concentrations of ELT. The net flux ratio of ELT decreased as the ELT concentration was increased (Figure 7B).

On the other hand, interaction of ELT with P-glycoprotein was not strong, since uptake of rhodamine123 in LLC-GA5-COL150 cells was minimally affected by ELT up to 10 μM, but was increased in the presence of a typical P-glycoprotein inhibitor, verapamil (Figure 6C). Uptake of rhodamine123 in LLC-GA5-COL150 cells was slightly increased by 30 μM ELT, but such an increase was also observed in LLC-PK1 cells (Figure 6C). Uptake of rosuvastatin (5 μM) and ELT (3 μM) was also evaluated in the present study, but there was no significant difference in uptake between the two cell lines (data not shown).

To evaluate the possible inhibition of BCRP-mediated secretion of rosuvastatin by ELT in humans, the plasma concentration of rosuvastatin was simulated using the PBPK model for the case that $F_a \cdot F_g$ of rosuvastatin was elevated to a value close to unity due to the inhibition of intestinal BCRP by ELT. On this assumption, the simulated plasma concentration of rosuvastatin was in good accordance with the clinical findings (Figure 2C).

DMD Fast Forward. Published on January 17, 2014 as DOI: 10.1124/dmd.113.054767
This article has not been copyedited and formatted. The final version may differ from this version.

DISCUSSION

Uptake of ELT by OATP1B1 was inhibited by several drugs in a concentration-dependent manner, and rosuvastatin and atorvastatin were the most potent inhibitors (Figure 1). IC_{50} values defined in terms of unbound concentration of rosuvastatin and atorvastatin were 1/7 ~ 1/8th of the respective unbound $C_{max,pv}$ (Table 2). Therefore, possible interaction between ELT and these statins cannot be ruled out. However, this seems incompatible with the clinical observation that there was no change in plasma concentration of ELT upon concomitant administration of rosuvastatin (Allred *et al.*, 2011). Prediction of drug interaction using $C_{max,pv}$ based on a so-called static model sometimes overestimates the interaction, yielding a false-positive prediction. Therefore, we focused on a more quantitative analysis using the PBPK model. This dynamic model (Figure S1) predicted that the plasma concentration profile of ELT would be only minimally changed after coadministration with rosuvastatin (Figure 2A), and this result was consistent with the clinical observation (Allred *et al.*, 2011). In addition, considering the previous report that a OATP1B1 inhibitor appears to be more potent *in vivo* than *in vitro* (Varma *et al.*, 2012), further simulation studies were performed by assuming 3~10 times more potent inhibition of OATP1B1 by rosuvastatin. Nevertheless, the AUC of ELT was estimated to increase only by at most 23% even when the Ki was set to be 1/10th of the IC_{50} experimentally obtained in the present study (Figure 2A). Thus, it is considered that inhibition of OATP1B1-mediated hepatic uptake of ELT by rosuvastatin would be minor.

On the other hand, ELT increases the plasma concentration of rosuvastatin in the clinical situation (Allred *et al*., 2011). Rosuvastatin is mainly excreted from liver (Martin *et al.*, 2003), and OATP1B1 plays an important role in hepatic uptake of rosuvastatin (Kitamura *et al.*, 2008). These reports implied that OATP1B1 could be possible primary target to explain the clinically observed ELT-rosuvastatin interaction. In fact, in the present study, ELT

DMD Fast Forward. Published on January 17, 2014 as DOI: 10.1124/dmd.113.054767
This article has not been copyedited and formatted. The final version may differ from this version.

inhibited uptake of rosuvastatin in both HEK293/OATP1B1 cells and human hepatocytes, the IC_{50} values being almost the same in both cases (Table 2). These results suggest that ELT potentially inhibits hepatic uptake of rosuvastatin via OTAP1B1. However, quantitative simulation using the PBPK model indicated that the plasma concentration of rosuvastatin in humans was only modestly affected by coadministration of ELT (Figure 2B). Thus, inhibition of OATP1B1-mediated hepatic uptake of rosuvastatin by ELT can account for only a part of the drug interaction. Sensitivity analysis was also performed by changing the K_i value (Figure 2B). The increase in AUC or C_{max} of rosuvastatin could be largely explained only if we assume that K_i *in vivo* is 1/3rd - 1/10th of the IC_{50} experimentally obtained *in vitro*. But, if we assume such potent inhibition of OATP1B1 by ELT, the time of maximum plasma concentration (T_{max}) was simulated to be prolonged, probably due to the inhibition of systemic clearance via OATP1B1 (Figure 2B). This is not in agreement with the clinical observation that T_{max} was minimally changed (Figure 2B, Allred *et al*. 2011).

Another possible target of ELT-rosuvastatin interaction could be an efflux transporter(s) for rosuvastatin in the liver and/or small intestine. Rosuvastatin is a substrate of BCRP, P-glycoprotein and multidrug resistance-associated protein 2 (Huang *et al.*, 2006; Kitamura *et al.*, 2008). Considering the minimal change in the terminal phase of the rosuvastatin profile caused by ELT (Figure 2B, Allred *et al.*, 2011), a plausible interaction mechanism could be inhibition of a small intestinal efflux transporter(s) for rosuvastatin by ELT. This hypothesis was supported by the present finding that triple gene knockout of *mdr1a/1b/bcrp* in rodents had a greater effect on the plasma rosuvastatin profile after oral administration (Figure 4A) than after intravenous administration (Figure 4B). It was also demonstrated in mouse intestinal loop that coadministration of ELT delayed absorption of rosuvastatin (Figure 5). Therefore, in the present study, possible inhibition by ELT of small-intestinal efflux transporters BCRP and P-glycoprotein was examined. ELT inhibited

DMD Fast Forward. Published on January 17, 2014 as DOI: 10.1124/dmd.113.054767
This article has not been copyedited and formatted. The final version may differ from this version.

BCRP-mediated rosuvastatin transport in MDCK/BCRP/PDZK1 cells, but had no effect in MDCK/mock/PDZK1 cells (Figure 6A), and the net flux ratio of rosuvastatin was decreased by 10 μM ELT (Figure 6B). In addition, ELT is transported by BCRP, and BCRP-mediated transport of ELT was saturated at ~10 μM ELT (Figure 7B). Tachibana *et al.* (2009) have proposed drug-interaction number (DIN) as an index of potential for inhibition of CYP3A4 and P-glycoprotein in small intestine. In the present study, we attempted to apply this theory to BCRP by using the IC_{50} for BCRP (Figure 6B) and the clinical dose of ELT. The apparent IC_{50} for BCRP was ~10 μM (Figure 6B), but this inhibitory effect of ELT was estimated in the presence of HSA. Therefore, we further considered the unbound fraction of ELT in the transport buffer containing HSA (~0.0072), and the IC_{50} defined in terms of unbound ELT concentration was estimated to be 0.07 μM. If we use this IC_{50} and the ELT dose (75 mg oral), the DIN is calculated to be more than 2,000 L. According to the criteria proposed by Tachibana *et al.* (2009), the risk of ELT-rosuvastatin interaction is therefore considered to be high, supporting the idea that the drug interaction is mediated by BCRP inhibition. Finally, rosuvastatin concentration in plasma was simulated based on the assumption that $F_a \cdot F_g$ is increased to a level close to unity by ELT-mediated inhibition of BCRP in small intestine. The simulation indicated that rosuvastatin concentration would be elevated to a level comparable with the clinical observation after coadministration with ELT (Figure 2C). This supports the conclusion that BCRP in the intestinal tract plays a key role in the interaction between rosuvastatin and ELT. It was reported that plasma concentration of rosuvastatin after oral administration is increased in patients with genetic polymorphism (421C>A) of *ABCG2* (Keskitalo *et al.*, 2009). BCRP in small intestine is considered to be primarily important for absorption of rosuvastatin since the AUC, but not elimination half-life, of rosuvastatin is increased by the gene polymorphism (Keskitalo *et al.*, 2009). Interestingly, the AUC of rosuvastatin after oral administration in patients with 421C>A *ABCG2* was approximately

DMD Fast Forward. Published on January 17, 2014 as DOI: 10.1124/dmd.113.054767
This article has not been copyedited and formatted. The final version may differ from this version.

twice that in individuals with the wild-type genotype (Keskitalo *et al.*, 2009). So, if we consider that the genetic polymorphism (421C>A) of *ABCG2* results in substantial loss of function of BCRP, the assumption in the present study (that $F_a \cdot F_g$ is increased from 0.5 to 0.9) is likely to be compatible with substantial inhibition of BCRP by ELT. However, such simple assumption may not be applied for other BCRP substrates since concentration of inhibitor drug in gastrointestinal tract should not be constantly high after its oral administration. In contrast to BCRP, inhibitory effect of ELT on P-glycoprotein could be less potent (Figure 6C). However, the inhibition study was performed up to 30 μM of ELT using rhodamine 123, but not rosuvastatin, as a substrate of P-glycoprotein. Thus, there could be limitations to this *in vitro* study that would underpredict the role of P-glycoprotein *in vivo*.

In the present study, we investigated the effect of drugs on OATP1B1-mediated ELT transport. The IC_{50} values of those drugs, other than rosuvastatin and atorvastatin, were higher than $C_{max,pv}$ (Table 2). One possible issue in the present study is that the transport buffer used to measure OATP1B1-mediated uptake of ELT contains HSA, and therefore the IC_{50} values for these compounds were defined based on the total concentration in the presence of HSA. Nevertheless, the HSA concentration (5 μM) used in the transport study was less than the physiological albumin concentration (~600 μM), so the unbound fraction in the transport study could be equal to or higher than that in human plasma. If IC_{50} is higher than $C_{max,pv}$ even under this condition, interaction of these drugs with OATP1B1-mediated hepatic uptake of ELT may be unlikely *in vivo*.

It has been reported that the plasma concentration profile of ELT is affected by genetic polymorphism (421C>A) of *ABCG2* (Allred *et al.*, 2011). In the present study, we demonstrated that ELT is a high-affinity substrate for BCRP, with saturation being observed at around 10 μM (Figure 7B). Thus, BCRP could be an important determinant of the pharmacokinetics of ELT. It is noteworthy that inhibition of BCRP by ELT occurred at the

clinical dose, implying that ELT may at least partially saturate small-intestinal BCRP. Therefore, further studies seem necessary to evaluate possible interaction of ELT with other orally administered BCRP substrate drugs.

The IC_{50} values for rosuvastatin and atorvastatin for OATP1B1-mediated ELT uptake (0.05 and 0.03 μM, respectively, Table 1) were much smaller than the K_m values for the uptake of these drugs by OATP1B1 (0.802 and 12.4 μM, respectively; Kitamura *et al*., 2008, Kameyama *et al*., 2005). This may imply that the substrate recognition site of OATP1B1 for ELT does not completely overlap with that for these typical OATP1B1 substrates, and the inhibition potential of other drugs for ELT uptake cannot be precisely predicted from uptake studies using other substrates than ELT itself. Therefore, drug interaction potential at OATP1B1 should be further examined in order to confirm the safety of pharmacotherapy using ELT.

ACKNOWLEDGEMENT

We thank Ms Lica Ishida for technical assistance and Ms Saki Umeda for fruitful discussions.

AUTHORSHIP CONTRIBUTINOS

Participated in research design: Takeuchi, Sugiura, Horikawa, Nakamichi, Ishiwata, Kato

Conducted experiments: Takeuchi, Matsubara, Sato, Shimizu,

Performed data analysis: Takeuchi, Sugiura, Matsubara

Wrote or contributed to the writing of the manuscript: Takeuchi, Sugiura, Masuo, Kato

REFERENCES

Allred AJ, Bowen CJ, Park JW, Peng B, Williams DD, Wire MB, and Lee E (2011) Eltrombopag increases plasma rosuvastatin exposure in healthy volunteers. *Br J Clin Pharmacol* **72**: 321-329.

Bauman JW, Vincent CT, Peng B, Wire MB, Williams DD and Park JW (2011) Effect of hepatic or renal impairment on eltrombopag pharmacokinetics. *J Clin Pharmacol* **51**: 739-750.

Bourdet DL, Pritchard JB, and Thakker DR (2005) Differential substrate and inhibitory activities of ranitidine and famotidine toward human organic cation transporter 1 (hOCT1; SLC22A1), hOCT2 (SLC22A2), and hOCT3 (SLC22A3). *J Pharmacol Exp Ther* **315**: 1288-1297.

Bussel JB, Cheng G, Saleh MN, Psaila B, Kovaleva L, Meddeb B, Kloczko J, Hassani H, Mayer B, Stone NL, Arning M, Provan D, and Jenkins JM (2007) Eltrombopag for the treatment of chronic idiopathic thrombocytopenic purpura. *N Engl J Med* **357**: 2237–2247.

Cheng G, Saleh MN, Marcher C, Vasey S, Mayer B, Aivado M, Arning M, Stone NL, Bussel JB (2011) Eltrombopag for management of chronic immune thrombocytopenia (RAISE): a 6-month, randomised, phase 3 study. *Lancet* **377**: 393-402.

Davies B and Morris T (1993) Physiological parameters in laboratory animals and humans. *Pharm Res* **10**: 1093-1095.

Deng Y, Madatian A, Wire MB, Bowen C, Park JW, Williams D, Peng B, Schubert E, Gorycki F, Levy M, and Gorycki PD (2011) Metabolism and disposition of eltrombopag, an oral, nonpeptide thrombopoietin receptor agonist, in healthy human subjects. *Drug Metab Dispos* **39**: 1734-1746.

Erickson-Miller L, Delorme E, Giampa L, Hopson C, Valoret E, Tian SS, Miller SG, Keenan

R, Rosen J, Dillon S, Duffy K, Lamb P, and Luengo J (2004) Biological activity and selectivity for TPO receptor of the orally bioavailable, small molecule TPO receptor agonist, SB-497115. *Blood (ASH Annual Meeting Abstracts)* **104**: 2912.

Erickson-Miller CL, Delorme E, Tian SS, Hopson CB, Landis AJ, Valoret EI, Sellers TS, Rosen J, Miller SG, Luengo JI, Duffy KJ, and Jenkins JM. (2008) Preclinical activity of eltrombopag (SB-497115), an oral, nonpeptide thrombopoietic growth factor. *Stem Cells* **27**: 424–430.

Fujioka T, Nara F, Tsujita Y, Fukushige J, Fukami M, and Kuroda M (1995) The mechanism of lack of hypocholesterolemic effects of pravastatin sodium, a 3-hydroxy-3-methylglutaryl coenzyme A reductase inhibitor, in rats. *Biochim Biophys Acta* **1254**: 7-12.

Fujita K, Sugiura T, Okumura H, Umeda S, Nakamichi N, Watanabe Y, Suzuki H, Sunakawa Y, Shimada K, Kawara K, Sasaki Y and Kato Y (2014) Direct inhibition and down-regulation by uremic plasma components of hepatic uptake transporter for SN-38, an active metabolite of irinotecan, in humans. *Pharm Res* **31**: 204-215.

Huang L, Wang Y, and Grimm S (2006) ATP-dependent transport of rosuvastatin in membrane vesicles expressing breast cancer resistance protein. *Drug Metab Dispos* **34**: 738-742.

Ito K, Iwatsubo T, Kanamitsu S, Ueda K, Suzuki H, and Sugiyama Y (1998) Prediction of pharmacokinetic alterations caused by drug-drug interactions: metabolic interaction in the liver. *Pharmacol Rev* **50**: 387-412.

Jenkins JM, Williams D, Deng Y, Uhl J, Kitchen V, Collins D, and Erickson-Miller CL (2007) Phase 1 clinical study of eltrombopag, an oral, nonpeptide thrombopoietin receptor agonist. *Blood* **109**: 4739–4741.

Jones HM, Barton HA, Lai Y, Bi YA, Kimoto E, Kempshall S, Tate SC, El-Kattan A, Houston

JB, Galetin A, and Fenner KS (2012) Mechanistic pharmacokinetic modeling for the prediction of transporter-mediated disposition in humans from sandwich culture human hepatocyte data. *Drug Metab Dispos* **40**: 1007-1017.

Kalliokoski A, Backman JT, Neuvonen PJ, and Niemi M (2008) Effects of the SLCO1B1*1B haplotype on the pharmacokinetics and pharmacodynamics of repaglinide and nateglinide. *Pharmacogenet Genomics* **18**: 937-942.

Kalliokoski A, Neuvonen PJ, and Niemi M (2010) SLCO1B1 polymorphism and oral antidiabetic drugs. *Basic Clin Pharmacol Toxicol* **107**: 775-781.

Kameyama Y, Yamashita K, Kobayashi K, Hosokawa M, and Chiba K (2005) Functional characterization of SLCO1B1 (OATP-C) variants, SLCO1B1*5, SLCO1B1*15 and SLCO1B1*15+C1007G, by using transient expression systems of HeLa and HEK293 cells. *Pharmacogenet Genomics*. **15**: 513-22.

Keskitalo JE, Zolk O, Fromm MF, Kurkinen KJ, Neuvonen PJ, and Niemi M (2009) ABCG2 polymorphism markedly affects the pharmacokinetics of atorvastatin and rosuvastatin. *Clin Pharmacol Ther* **86**: 197-203.

Kimura N, Masuda S, Tanihara Y, Ueo H, Okuda M, Katsura T, and Inui K (2005) Metformin is a superior substrate for renal organic cation transporter OCT2 rather than hepatic OCT1. *Drug Metab Pharmacokinet* **20**: 379-386.

Kitamura S, Maeda K, Wang Y, and Sugiyama Y (2008) Involvement of multiple transporters in the hepatobiliary transport of rosuvastatin. *Drug Metab Dispos* **36**: 2014-2023.

Martin PD, Warwick MJ, Dane AL, Brindley C, and Short T (2003) Absolute oral bioavailability of rosuvastatin in healthy white adult male volunteers. *Clin Ther* **25**: 2553-2563.

Sellers T, Hart T, Semanik M, and Murthy K (2004) Pharmacology and safety of SB-497115-GR, an orally active small molecular weight TPO receptor agonist, in

chimpanzees, rats and dogs. *Blood* **104**: 2063a.

Shimizu T, Sugiura T, Wakayama T, Kijima A, Nakamichi N, Iseki S, Silver DL, and Kato Y (2011) PDZK1 regulates breast cancer resistance protein in small intestine. *Drug Metab Dispos* **39**: 2148-54.

Stasi R and Provan D (2004) Management of immune thrombocytopenic purpura in adults. *Mayo Clin Proc* **79**: 504-522.

Sugiura T, Otake T, Shimizu T, Wakayama T, Silver DL, Utsumi R, Nishimura T, Iseki S, Nakamichi N, Kubo Y, Tsuji A, Kato Y (2010) PDZK1 regulates organic anion transporting polypeptide Oatp1a in mouse small intestine. *Drug Metab Pharmacokinet* **25**: 588-598.

Tachibana T, Kato M, Watanabe T, Mitsui T, and Sugiyama Y (2009) Method for predicting the risk of drug-drug interactions involving inhibition of intestinal CYP3A4 and P-glycoprotein. *Xenobiotica* **39**: 430-443.

Takeuchi K, Sugiura T, Umeda S, Matsubara K, Horikawa M, Nakamichi N, Silver DL, Ishiwata N, and Kato Y (2011) Pharmacokinetics and hepatic uptake of eltrombopag, a novel platelet-increasing agent. *Drug Metab Dispos* **39**: 1088-1096.

Tanigawara Y, Okamura N, Hirai M, Yasuhara M, Ueda K, Kioka N, Komano T, Hori R (1992) Transport of digoxin by human P-glycoprotein expressed in a porcine kidney epithelial cell line (LLC-PK1). *J Pharmacol Exp Ther* **263**: 840–845.

Ueda K, Okamura N, Hirai M, Tanigawara Y, Saeki T, Kioka N, Komano T, Hori R (1992) Human P-glycoprotein transports cortisol, aldosterone, and dexamethasone, but not progesterone. *J Biol Chem* **267**: 24248–24252.

Varma MV, Lai Y, Feng B, Litchfield J, Goosen TC, and Bergman A (2012) Physiologically based modeling of pravastatin transporter-mediated hepatobiliary disposition and drug-drug interactions. *Pharm Res* **29**: 2860-73.

Watanabe T, Kusuhara H, Maeda K, Shitara Y, and Sugiyama Y (2009) Physiologically based pharmacokinetic modeling to predict transporter-mediated clearance and distribution of pravastatin in humans. *J Pharmacol Exp Ther* **328**: 652-662.

Wire MB, McLean HB, Pendry C, Theodore D, Park JW, Peng B (2012) Assessment of the pharmacokinetic interaction between eltrombopag and lopinavir-ritonavir in healthy adult subjects. *Antimicrob Agents Chemother* **56**: 2846-2851.

FOOTNOTES

This study was supported in part by a Grant-in-Aid for Scientific Research provided by the Ministry of Education, Science and Culture of Japan, and a grant from the Naito Foundation (Tokyo, Japan), in part by Shimabara-kagaku Foundation (Tokyo, Japan) and in part by the Advanced Research for Medical Products Mining Programme of the National Institute of Biomedical Innovation (NIBIO).

DMD Fast Forward. Published on January 17, 2014 as DOI: 10.1124/dmd.113.054767
This article has not been copyedited and formatted. The final version may differ from this version.

LEGENDS TO FIGURES

Figure 1. Effect of therapeutic agents on ELT uptake by HEK293/OATP1B1 cells

HEK293/OATP1B1 cells were incubated with ELT (10 μM) for 30 min at 37˚C in the absence or presence of various therapeutic agents for ITP (panel A) including prednisolone (●), clarithromycin (◆), amoxicillin (▲), omeprazole (■), rabeprazole (○), lansoprazole (◇), azathioprine (△), and cyclophosphamide (□) and those for lifestyle diseases (panel B) including rosuvastatin (●), atorvastatin (◆), pravastatin (▲), repaglinide (○), glibenclamide (◇), and nateglinide (△). Transport buffer containing 5 μM HSA was used in order to prevent non-specific adsorption of ELT. OATP1B1-mediated uptake was calculated by subtraction of the uptake observed in HEK293/mock cells from that in HEK293/OATP1B1 cells, and normalized by the uptake in the absence of inhibitors. Each value represents the mean±S.E.M. (n=6-15).

Figure 2. Fitting and simulation of plasma concentration profile of ELT (A) and rosuvastatin (B, C) when these drugs are administered alone or together

Closed circle represents clinical data previously obtained when ELT (75 mg) or rosuvastatin (10 mg) was orally administered alone, while dotted lines represent those previously obtained when both drugs were simultaneously administered (Allred *et al.*, 2011). Solid lines in panels (A) and (B) represent fitted ones to the PBPK model shown in Figure S1. Broken lines in panels (A) and (B) represent simulated profiles after co-administration of both drugs when we consider the interaction at OATP1B1 for the cases where Ki was set to be the same as IC_{50} obtained in HEK293/OATP1B1 cells, or 1/3 and 1/10 of that value. Broken lines in panel (C) represent the simulated profiles after co-administration of both drugs when we consider the interaction at BCRP in the small intestine, and $F_a \cdot F_g$ is assumed to be 0.9. Note that the broken line (IC_{50}) in panel (A) is unclear because it is almost superimposed on the

solid line.

Figure 3. Effect of ELT on uptake of rosuvastatin by human hepatocytes (A) and OATP1B1 (B) and effect of ELT on OCT1-mediated drug uptake (C)

(A, B) In panel (A), human hepatocytes were incubated with rosuvastatin (1 μM) for 10 min at 37˚C in the absence or presence of ELT. In panel (B), HEK293/OATP1B1 cells were incubated with rosuvastatin (1 μM) for 5 min at 37˚C in the absence or presence of ELT. OATP1B1-mediated uptake was calculated by subtraction of the uptake in HEK293/mock cells from that in HEK293/OATP1B1 cells. In panels (A) and (B), the uptake was examined in the absence of HSA, and ELT concentration shown on the abscissa represents that experimentally measured. Each value represents the mean±S.E.M. (n=3-6).

(C) HEK293/OCT1 cells were incubated with the transport buffer containing 5 μM HSA and metformin (3 mM, 30 min, ●), ranitidine (30 μM, 15 min, ◆) or cimetidine (30 μM, 15 min, ▲) at 37°C in the absence or presence of ELT. OCT1-mediated uptake was calculated by subtraction of the uptake in HEK293/mock cells from that in HEK293/OCT1cells. Each value represents the mean±S.E.M. (n=6-12).

Figure 4. Involvement of two ABC transporters in gastrointestinal absorption of rosuvastatin and ELT in mice

(A, B) Plasma concentration-time profiles of rosuvastatin were measured after oral administration (10 mg/kg, A) and *i.v.* bolus injection (4 mg/kg, B) in wild-type (open circles) and *mdr1a/1b/bcrp*$^{-/-}$ (closed circles) mice. Each value represents the mean ± S.E.M. (n = 3).

(C) Plasma concentration-time profiles of ELT was measured after oral administration of ELT (1 mg/kg) in wild-type (open circles) and *mdr1a/1b/bcrp*$^{-/-}$ (closed circles) mice. Each value represents the mean ± S.E.M. (n = 5-6).

Figure 5. Interaction of ELT with rosuvastatin in small intestine in mice

Plasma concentration-time profiles of rosuvastatin were measured in wild-type mice after injection into an intestinal loop of rosuvastatin (10 mg/kg) with (closed circles) or without (open circles) ELT (2 mg/kg). Each value represents the mean ± S.E.M. (n = 3-8).

Figure 6. Inhibition by ELT of BCRP-mediated transport of rosuvastatin (A, B), but minimal effect of ELT on P-glycoprotein (C)

(A) Transcellular transport of rosuvastatin (5 μM) in the apical-to-basal direction was measured across MDCKII/BCRP/PDZK1 (closed symbols) and MDCKII/Mock/PDZK1 cells (open symbols) in the presence (triangles) or absence (circles) of ELT (10 μM). Each value represents the mean ± S.E.M. (n = 3-12).

(B) Transcellular transport of rosuvastatin was measured in the absence or presence of various concentrations of ELT in both MDCKII/BCRP/PDZK1 and MDCKII/Mock/PDZK1 cells, and the net flux ratio of rosuvastatin was calculated. Each value represents the mean ± S.E.M. (n = 3-6).

(C) Uptake of rhodamine123 (5 μM) was measured in the absence or presence of ELT or P-glycoprotein inhibitor verapamil (VER) in LLC-PK1 (open bar) and LLC-GA5-COL150 (closed bar). The uptake was then normalized by medium concentration and is shown as distribution volume (n = 7-12).

Figure 7. Saturable transport of ELT by BCRP

(A) Transcellular transport of ELT (1 μM) in the apical-to-basal direction was measured in MDCKII/BCRP/PDZK1 (closed symbols) and MDCKII/Mock/PDZK1 cells (open symbols) in the presence (triangles) or absence (circles) of BCRP inhibitor Ko143 (1 μM). Each value

represents the mean ± S.E.M. (n = 3-9).

(B) Transcellular transport of ELT was measured at various concentrations in both MDCKII/BCRP/PDZK1 and MDCKII/Mock/PDZK1 cells, and the net flux ratio of ELT was calculated. Each value represents the mean ± S.E.M. (n = 3-9).

Table 1 Pharmacokinetic parameters for ELT and rosuvastatin

Parameter	ELT	Rosuvastatin
$F_a \cdot F_g$	0.5 [a]	0.543 [b]
k_a (min^{-1})	0.0084 [e]	0.0046 [e]
R_b [f]	0.718 [a]	0.69 [b]
f_p [g]	0.002 [a]	0.12 [b]
V_d (L)	2.94 [e]	245 [e]
PS_{inf} (mL/min)	3250 [e]	10100 [e]
CL_{NH} (mL/min)	0	330 [b]
Q_h (mL/min)	1450 [c]	
V_{extra} [h] (mL)	469 [d]	
V_{liver} [i] (mL)	1690 [c]	

a) Cited from FDA Pharmacology Review of Promacta.
b) Cited from Martin et al., 2003.
c) Cited from Davies and Morris, 1993.
d) Cited from Watanabe et al., 2009.
e) Estimated by fitting in the present study.
f) Blood-to-plasma partition ratio
g) Unbound fraction in plasma
h) Volume of extracellular space in liver
i) Volume of liver

DMD Fast Forward. Published on January 17, 2014 as DOI: 10.1124/dmd.113.054767
This article has not been copyedited and formatted. The final version may differ from this version.

Table 2. IC_{50} for the inhibition by therapeutic agents of OATP1B1-mediated uptake of ELT or rosuvastatin, and their clinically effective concentration

Substrate	Therapeutic agent	IC_{50} [a] (μM)	$C_{max,sys}$ [b] (μM)	$C_{max,pv}$ [c] (μM)
ELT	Rosuvastatin[d]	0.062 (0.047)	0.046 (0.0055)	2.9 (0.35)
	Atorvastatin[d]	0.047 (0.028)	0.049 (0.0021)	5.0 (0.22)
	Pravastatin[e]	>100	0.072	3.2
	Repaglinide[e]	3.4	0.061	0.061
	Nateglinide[e]	96	31	50
	Glibenclamide[e]	73	0.089	0.79
	Prednisolone[e]	>100	1.8	9.5
	Clarithromycin[e]	>100	3.0	40
	Amoxicillin[e]	>100	24	40
	Omeprazole[e]	>100	3.3	11
	Rabeprazole[e]	>100	1.1	4.7
	Lansoprazole[e]	>100	2.8	8.4
	Azathioprine[e]	>100	7.2	32
	Cyclophosphamide[e]	>100	22	84
Rosuvastatin	ELT[d]	0.090	29 (0.029)	41 (0.041)

a) Estimated in HEK293/OATP1B1 cells in the present study.
b) Maximum plasma concentration cited from the interview forms. Values in parenthesis represent unbound concentration, which was calculated as $f_p \cdot C_{max,sys}$.
c) The maximum concentration at the inlet to liver was calculated using Eq. (3). Values in parenthesis represent unbound concentration, calculated as $f_p \cdot C_{max,pv}$.
d) Protein binding in the uptake study for these compounds was experimentally determined, and the IC_{50} values in parenthesis were defined in terms of unbound concentration.
e) For these compounds, IC_{50}, $C_{max,sys}$ and $C_{max,pv}$ were defined in terms of total concentration.

Figure 1

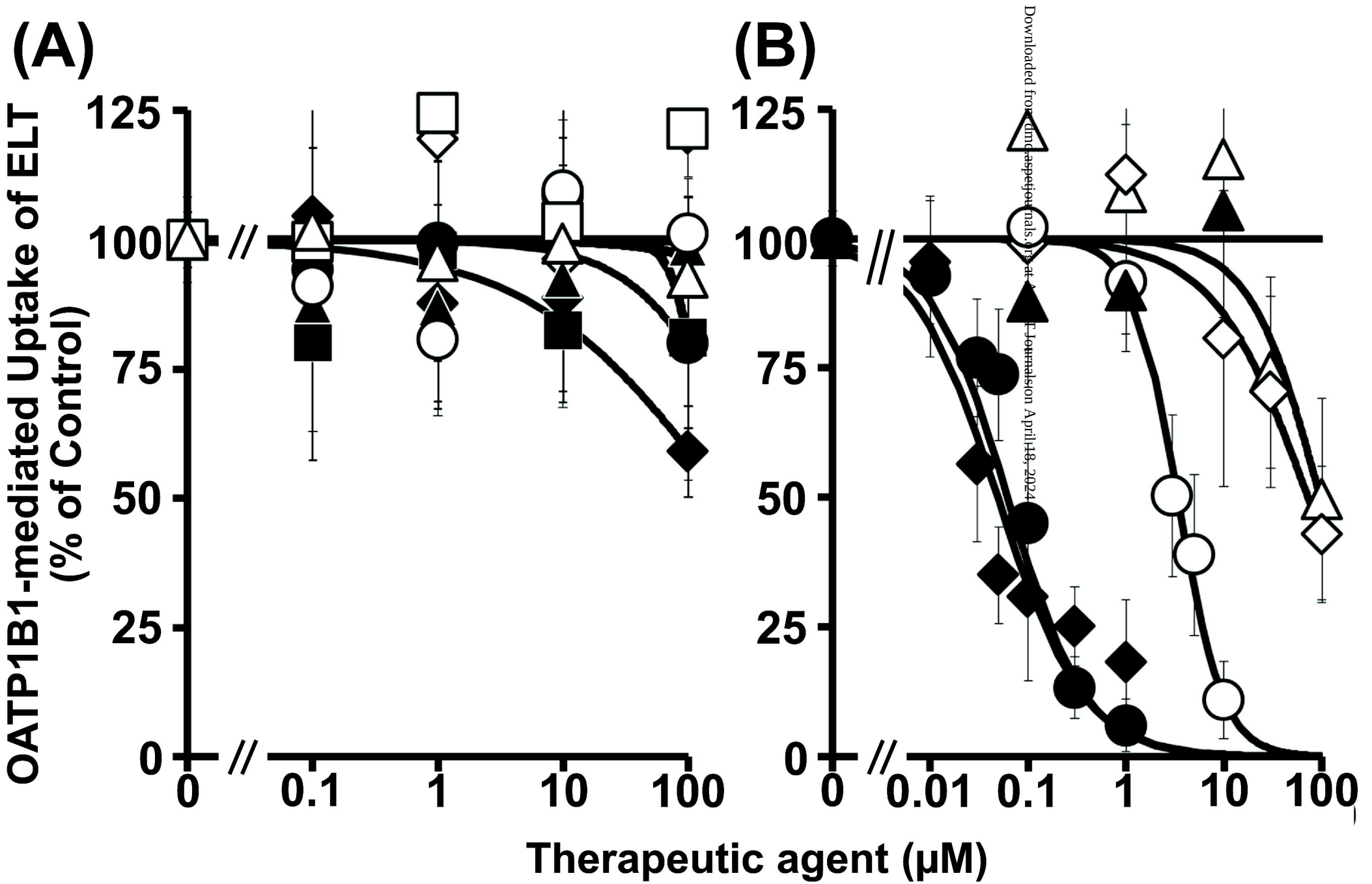

Figure 2

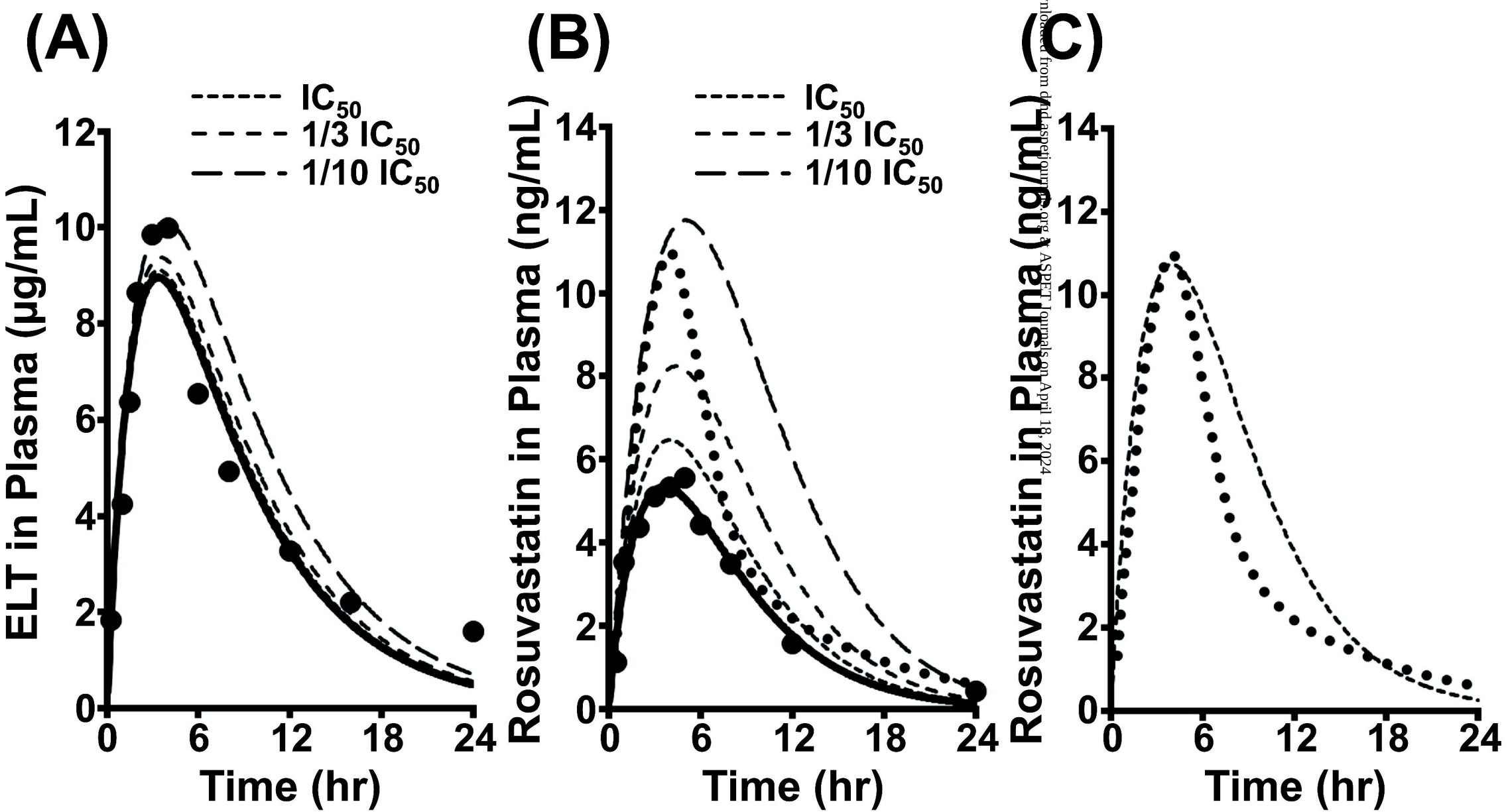

Figure 3

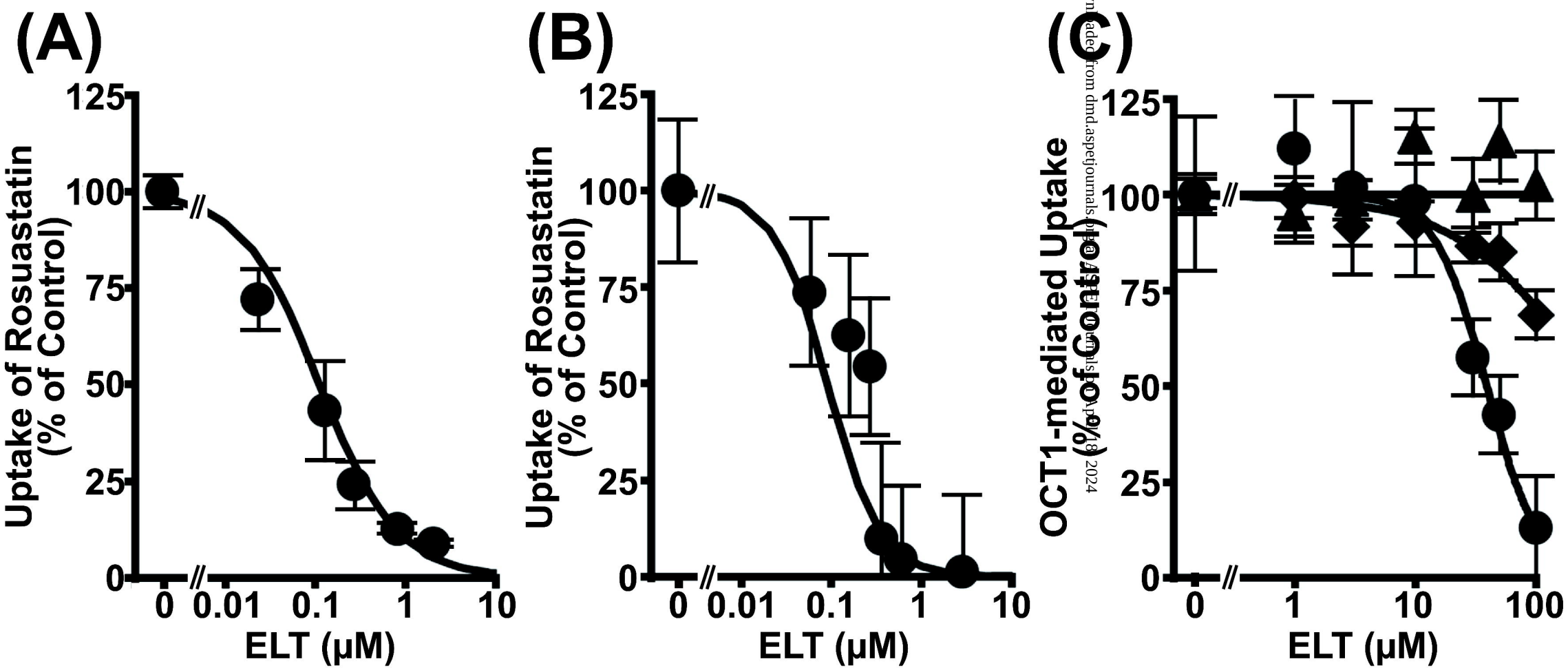

Figure 4

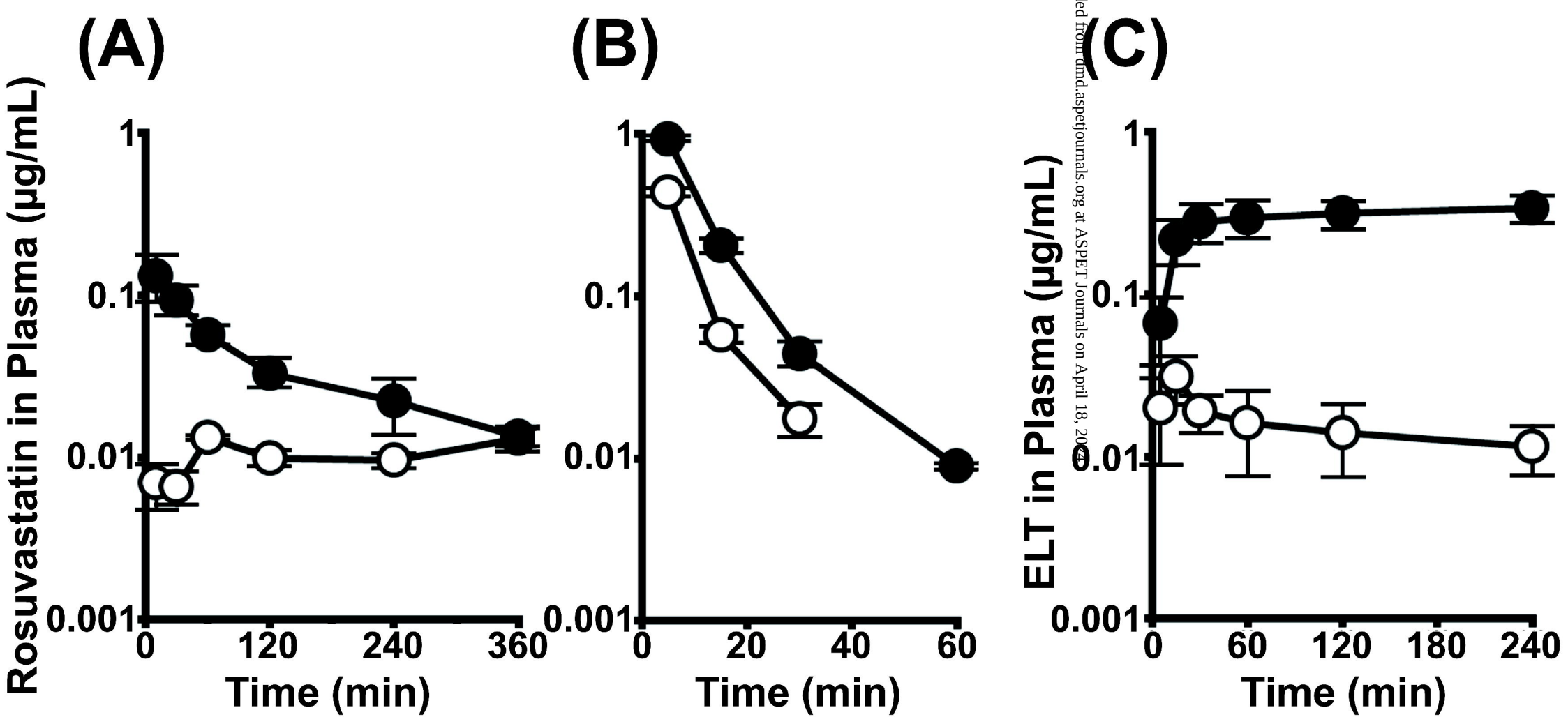

Figure 5

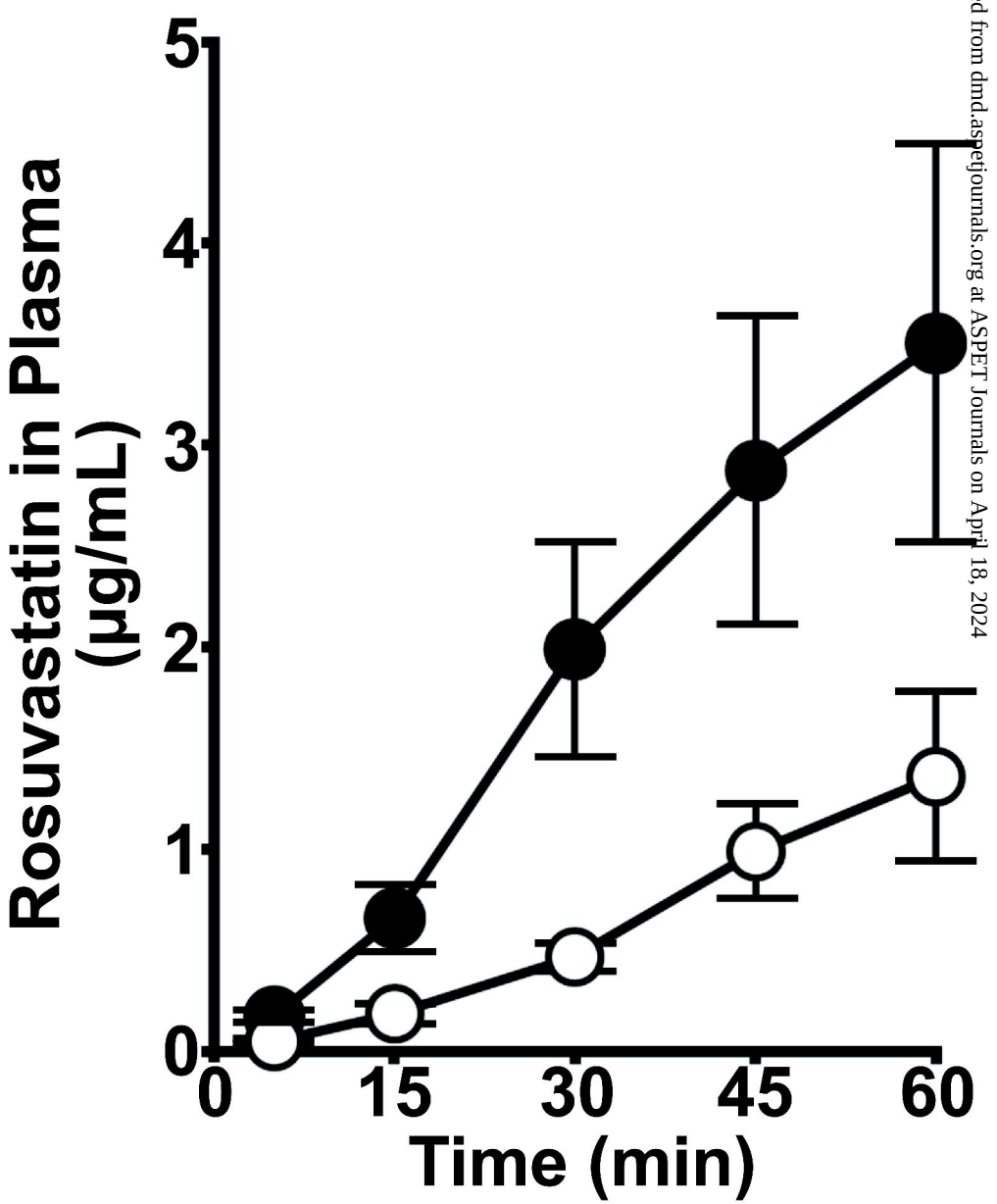

Figure 6

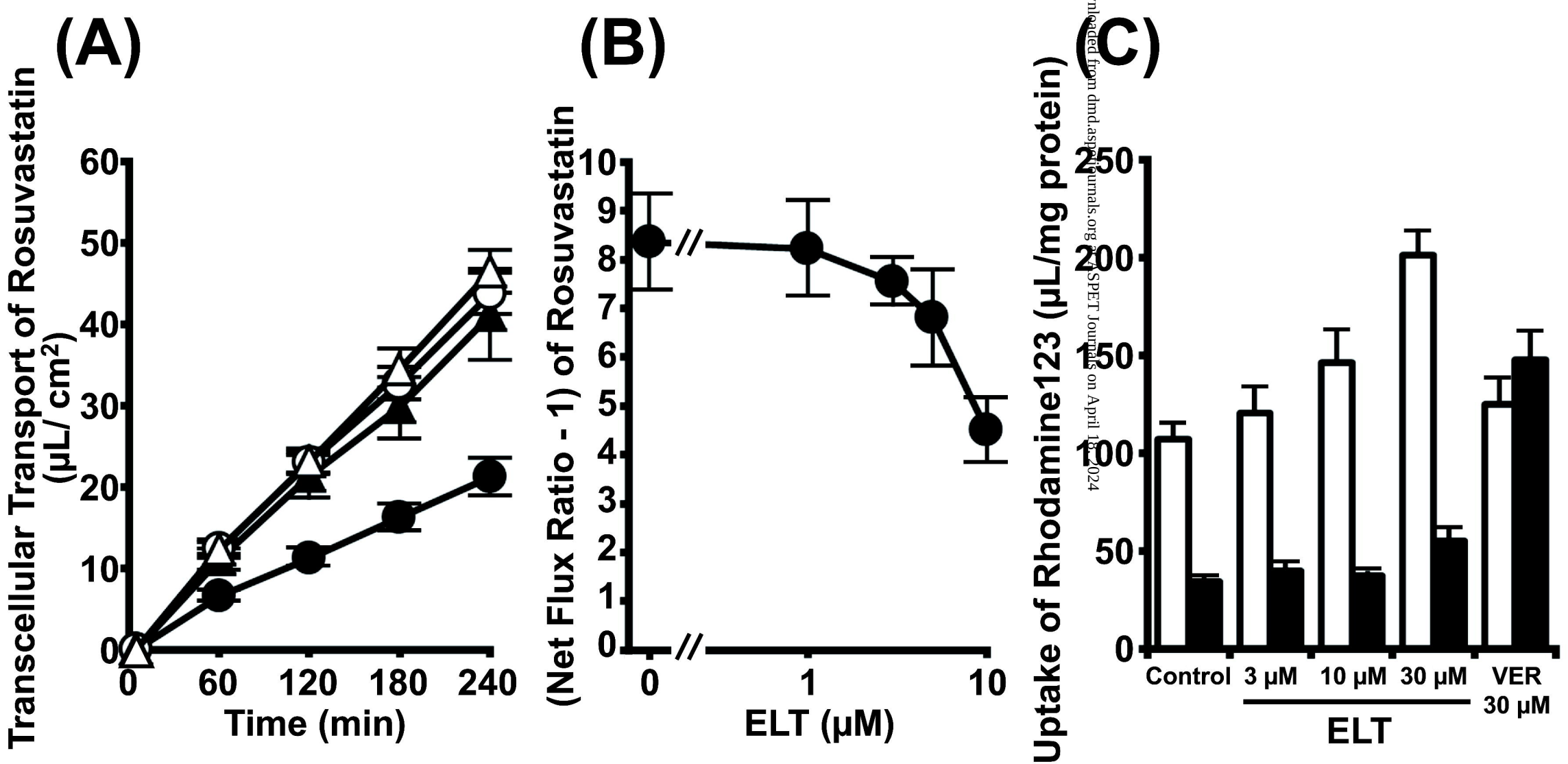

Figure 7